

PAPER • OPEN ACCESS

## Influence of joule heat and heat of electric arc on the vortex flow in DC arc furnace

To cite this article: O V Kazak and I O Starodumov 2020 *IOP Conf. Ser.: Mater. Sci. Eng.* **709** 044032

View the [article online](#) for updates and enhancements.



**LIVE AWARDS AND SPECIAL EVENTS**

**PLENARY LECTURE:**  
"Perovskite Solar Cells: Past 10 Years and Next 10 Years" with *Nam-Gyu Park*

**LEGENDS OF BATTERY SCIENCE:**  
A Celebration with *M. Stanley Whittingham* and *Akira Yoshino*

**PRiME 2020 • October 4-9, 2020**  
*Hosted daily: 2000h ET & 0900h JST/KST*

**PRIME<sup>TM</sup>**  
PACIFIC RIM MEETING  
ON ELECTROCHEMICAL  
AND SOLID STATE SCIENCE  
**2020**

**ATTENDEES  
REGISTER FOR FREE ▶**

# Influence of joule heat and heat of electric arc on the vortex flow in DC arc furnace

**O V Kazak\* and I O Starodumov**

Laboratory of Multi-Scale Mathematical Modeling, Ural Federal University,  
Ekaterinburg, Russia

\* olegkazak@yandex.ru

**Abstract.** The paper devoted to the numerical simulation of processes in DC electric arc furnaces with the bottom electrode. These furnaces have shown higher efficiency, low heat loss, lower components wear and higher quality of steel production. The biggest disadvantage of such furnaces is a high rate of fettle wear near the bottom electrode that connected with electrovortex flow. Electrovortex flows appearing under electromagnetic forces as a result of non-homogeneous distribution of the current density through the liquid conductor. This effect can be observed in many technological processes: electro slag remelting process (including DC and AC metallurgical furnaces, electrolysis cells and submerged-resistor induction furnaces), arc welding, processes of semiconductor crystals growing, electro vortex engines etc.

## 1. Introduction

The modern metallurgical industry needs new safety and low energy consuming steelmaking technology. The DC arc furnace is one of such technology. DC arc furnace has shown many advantages in compare with AC arc furnaces [1]. In this work the physical and mathematical model of processes proceeding in DC arc furnace has been build [2,3]. It takes into account the spatial distribution of the current, electric and magnetic fields, temperature, Lorenz force, joule heat and convection. The strategy of solving the stated conjugate problem in standard software packages is worked out. Numerical simulation of proceeding processes in liquid metal for DC arc furnace with different parameters is carried out. One of the most important problems of DC arc furnace is a high rate of fettle wear near the bottom electrode that connected with electrovortex flow [4]. Electrovortex flows appearing under electromagnetic forces as a result of non-homogeneous distribution of the current density through the liquid conductor. This effect can be observed in many technological processes: electro slag remelting process (including DC and AC furnaces, electrolysis cells and submerged-resistor induction furnaces), arc welding, processes of semiconductor crystals growing, electro vortex engines etc. [5]. That is why it is important to know intensity of electrovortex flow in every period of DC arc furnace working and influence of all parameters on the electrovortex flow intensity.

## 2. Presentation of the problem and model for numerical simulation

The operation period of DC arc furnace with a bottom electrode can be divided into the following stages: the melting of the burden, the liquid period when steel is produced, and tapping. The liquid period covers from 15% to 60% of the entire period depending on the steel type produced and the



Content from this work may be used under the terms of the [Creative Commons Attribution 3.0 licence](https://creativecommons.org/licenses/by/3.0/). Any further distribution of this work must maintain attribution to the author(s) and the title of the work, journal citation and DOI.

quality of the initial raw material [6-7]. It is essential that the processes in DC arc furnace during the liquid period are estimated.

In this type of furnace, the vortex flow of the liquid metal is the result of the spatial unevenness of the current in the absence of an outer magnetic field. The current in the liquid creates a magnetic field of its own, which causes the liquid's vortex movement.

Convection flows make their own contribution to the vortex flow and appear with an uneven distribution of the temperature throughout the liquid volume. It is shown in [5] that the heat convection in an electrovortex flow with axial symmetry appears when a radial gradient exists ( $\partial T / \partial r \neq 0$ ). The direction of convection depends on the increase or decrease of the temperature value with the increase of the distance from the axis of symmetry.

During the liquid period, the temperature difference throughout the metal volume can range depending on the mode of the furnace operation. Thus, when the arc works at full power the temperature ranges from 3773 K in the arc area at the cathode to 1923 K in the bottom electrode area and along the fettle surface. At low power, the temperature difference throughout the metal volume does not exceed 50 K. It should be noted that the metal during this period is liquid.

The velocity of the liquid that appears under electromagnetic force can be estimated as  $u_0 = j_0 L \sqrt{\mu_0 / \rho} \approx 0.3 \text{ m/s}$  [5]. The Grashof number that defines the ratio of the relative intensity of convection depending on the temperature range and electrovortex flow in the furnace is ranged in different periods from  $Gr = 0.5 < 1$  (low power) to  $Gr = \beta \Delta T g L / u_0^2 \approx 18.5 > 1$  (full power). This corresponds to the insignificant or essential contribution of the convection to the general vortex flow [5]. According to the preliminary estimates, during the period when the arc is at full power it is necessary to take convection into account: however, convection can be neglected when the arc is at low power.

The relative power of Joule heating as compared with another heat source (heat from the arc) is low:

$$Q = \frac{j_0^2 L}{\sigma \rho c u_0 \Delta T} \approx 10^{-3} \ll 1. \text{ This means the arc heat is more intense than joule heating [5].}$$

The Peclet number that defines the ratio of free heat convection transfer to molecule heat conduction equals  $Pe = u_0 L / \chi \approx 10^5 \gg 1$ . This means that heat convection is dominant over molecule heat conduction [5].

The magnetic Reynolds number is part of the magnetic induction equation. The magnetic Reynolds number is low in this problem ( $Re_m = \mu_0 \sigma u_0 L \approx 0.4 < 1$ ), meaning that the movement of the liquid conductor does not change the magnetic field and the calculation can be carried out via a non-induction approximation [5].

The processes in the DC EAF during metal smelting are not steady. However, they are rather slow and can be described via quasisteady or steady formulations. For a steady statement, the molten metal movement in the furnace can be described by the system of equations for magnetic, heat transfer, and hydrodynamic processes.

The electromagnetic processes in liquid metal can be described by Maxwell's equations:

$$\nabla \times \vec{B} = \mu_0 \vec{j}, \nabla \cdot \vec{B} = 0, \quad (1)$$

$$\nabla \times \vec{E} = 0, \nabla \cdot \vec{E} = \frac{\rho_e}{\epsilon_0}, \quad (2)$$

Ohm's law for fluid in motion:

$$\vec{j} = \sigma (\vec{E} + \vec{u} \times \vec{B}) \quad (3)$$

and charge conservation law:

$$\nabla \cdot \vec{j} = 0, \quad (4)$$

where  $\vec{j}$  – current density,  $\rho_e$  – charge density,  $\vec{B}$  – magnetic induction intensity vector,  $\vec{E}$  – electrical field intensity,  $\sigma$  – specific conductance,  $\mu_0$  – permeability of free space,  $\varepsilon_0$  – permittivity of free space,  $\vec{u}$  – liquid velocity.

The heat parameters are calculated by the heat transfer equation

$$\rho C_p \vec{u} \cdot \nabla T = \nabla \cdot ((a + a_T) \nabla T) + j^2 / \sigma, \quad (5)$$

where  $\rho$  – density,  $C_p$  – specific heat,  $T$  – temperature,  $a$  – heat conduction coefficient,  $a_T$  – turbulent heat conduction coefficient,  $j^2 / \sigma$  – Joule heat source.

The hydrodynamic processes in the liquid can be described by the Navier-Stokes equation

$$\rho \vec{u} \cdot \nabla \vec{u} = \nabla \cdot (-pI + (\nu + \nu_T)(\nabla \vec{u} + (\nabla \vec{u})^T)) - (2/3)(\nabla \cdot \vec{u})I + \rho \vec{g} + \vec{j} \times \vec{B}; \quad (6)$$

and the equation of continuity

$$\nabla \cdot (\rho \vec{u}) = 0, \quad (7)$$

where  $p$  – pressure,  $\vec{g}$  – gravitation,  $\nu = \eta / \rho$  – coefficient of kinematics viscosity,  $\eta$  – coefficient of dynamic viscosity,  $\rho$  – liquid density,  $I$  – identity operator for points on the boundary. The following forces are considered in equation (6):  $-\nabla \cdot p$  – pressure force;  $\nabla \cdot (\nu + \nu_T)(\nabla \vec{u} + (\nabla \vec{u})^T)$  – force of viscous friction;  $\vec{j} \times \vec{B}$  – Lorentz electromagnetic force.

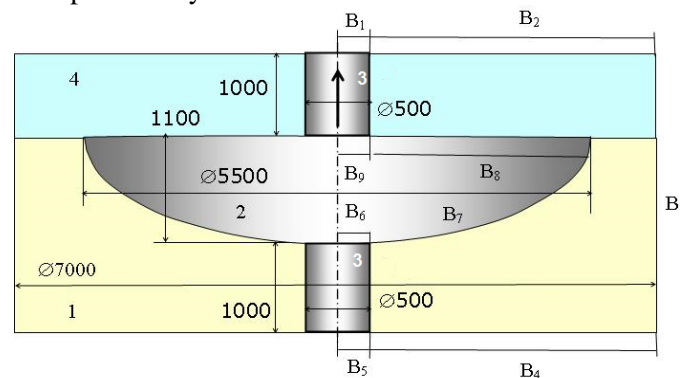
According to the preliminary estimation the Reynolds number under the movement in DC EAF is  $Re = u_0 L / \nu \approx 10^6$ , which is equivalent to the developed turbulent flow that can be described within  $k - \varepsilon$  turbulence model.

The formulated problem was solved with the corresponding boundary conditions that are defined in Figure 1 as B<sub>1</sub>-B<sub>9</sub> as for the model of real DC arc furnace [8].

Electromagnetic conditions: B<sub>1</sub>, B<sub>5</sub>, B<sub>6</sub>, B<sub>9</sub> – current density on the boundary with normal cross-section of electrode  $\vec{j}_n = \vec{j}_0 = I/S$ , where  $S$  is the cross section of electrode; B<sub>8</sub>, B<sub>7</sub> – current insulation  $\vec{j}_n = 0$ ; B<sub>6</sub>, B<sub>7</sub>, B<sub>8</sub>, B<sub>9</sub> – the conditions of continuity of electric and magnetic fields:  $E_{r_1} = E_{r_2}$ ,  $D_{n_1} = D_{n_2}$  and  $B_{n_1} = B_{n_2}$ ,  $B_{r_1} = B_{r_2}$ .

Heat conditions: B<sub>9</sub> – constant temperature of electric arc  $T_1 = 3300$  K; B<sub>6</sub> – constant temperature on bottom electrode  $T_2 = 1980$  K; B<sub>8</sub> – constant temperature on boundary with slag  $T_3 = 1900$  K; B<sub>7</sub> – constant temperature on boundary with fettle  $T_3 = 1900$  K.

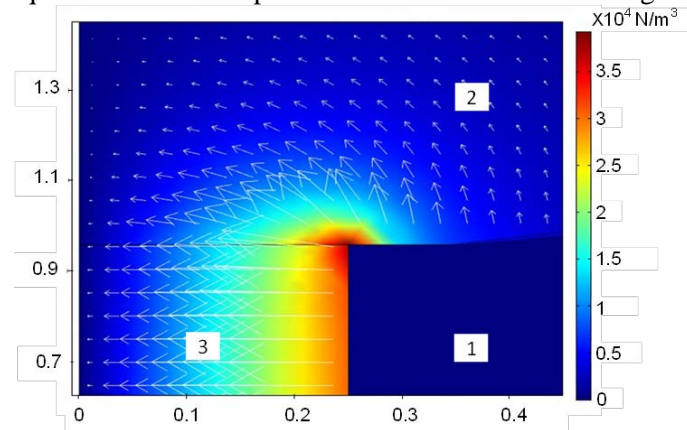
Hydrodynamic conditions: B<sub>6</sub>, B<sub>7</sub>, B<sub>8</sub>, B<sub>9</sub> – the no-slip boundary condition on all boundaries of liquid was used, both on the boundary of the liquid with the fettle and the boundary of liquid with slag. The last approximation is based on the fact that slag viscosity is much higher than liquid viscosity and it can be considered as no-slip boundary condition.



**Figure 1.** Arrangement and dimensions of the researched cylindrical DC EAF (1– fettle, 2 – liquid metal, 3 – top and bottom electrodes, 4 – slag)

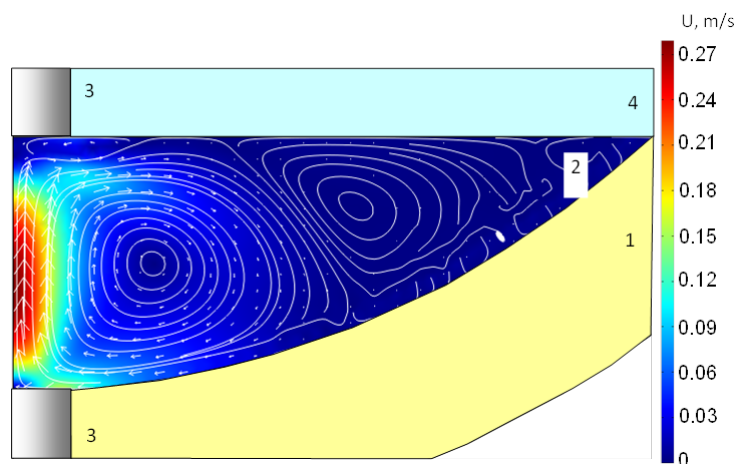
### 3. Selected numerical results

Some simulation results of the processes proceeding in liquid steel are given below. Figure 2 demonstrates the vector and contour fields of the Lorentz force density near the bottom electrode (anode). The value of Lorentz force ranged up to  $3.5 \cdot 10^4 \text{ N/m}^3$  close to the interface between fettle, bottom electrode and liquid metal and comprised about 30 % of volumetric gravity force.



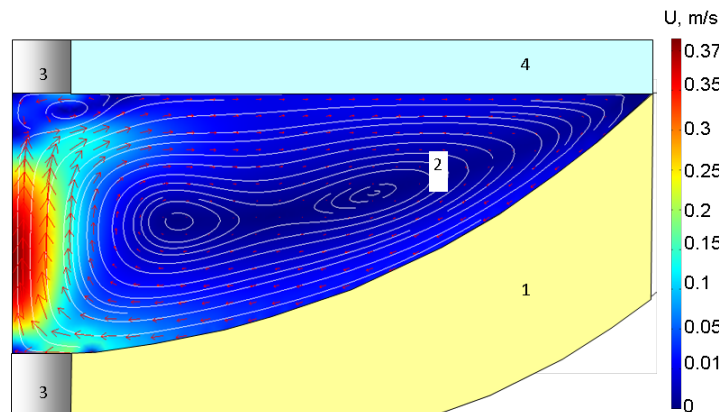
**Figure 2.** The vector and contour field of the Lorentz force density near the bottom electrode (1 – fettle, 2 – liquid metal, 3 – top and bottom electrodes, 4 – slag).

Figure 3 demonstrates hydrodynamic fields of velocity vector, contour and streamlines. The higher intensity of vortex flows appears in liquid metal volume. In this case we can see electrovortex flow produce only by electromagnetic force without convection. The maximum velocity value arise 0.27 m/s in the symmetry axis.



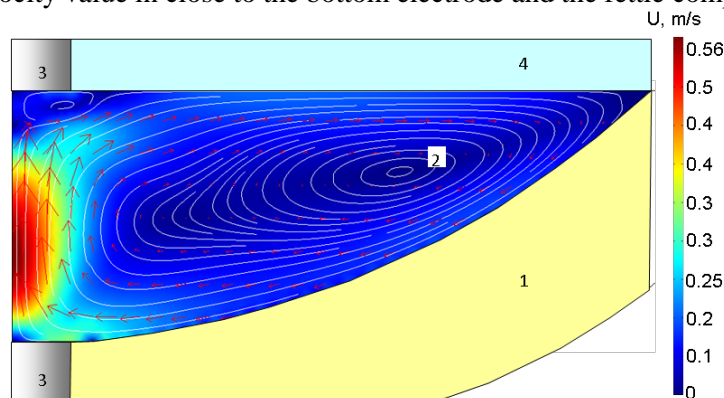
**Figure 3.** The vector, contour field and streamlines of velocity without convection (1 – fettle, 2 – liquid metal, 3 – top and bottom electrodes, 4 – slag).

Figure 4 demonstrates flow under electromagnetic force and convection flows under joule heat from the electric current flow in the liquid metal. This case arises when top electrode located in the liquid metal and don't produce electric arc between electrode and liquid metal. The convection flows are in the line with electrovortex flows and the total vortex flow increases. The maximum value of the vortex flow velocity was located on the axis of symmetry and reaches 0.37 m/s. The vortex flow velocity value in close to the bottom electrode and the fettle comprises about 0.2 m/s.



**Figure 4.** The vector, contour field and streamlines of velocity with convection (1 – fettle, 2 – liquid metal, 3 – top and bottom electrodes, 4 – slag).

Figure 5 demonstrates flow under electromagnetic force and convection flows with takes into account total joule heat from the electric current in liquid metal and heat that produce electric arc. The maximum value of the vortex flow velocity was located on the axis of symmetry and reaches 0.56 m/s. The vortex flow velocity value in close to the bottom electrode and the fettle comprises about 0.3 m/s



**Figure 5.** The vector, contour field and streamlines of velocity with convection (1 – fettle, 2 – liquid metal, 3 – top and bottom electrodes, 4 – slag).

#### 4. Conclusions

The work offers on the basis of numerical simulation of the hydrodynamic fields of velocity vector, contour and streamlines taking into account the Lorentz force distribution in the liquid metal, heat producing by joule heat in liquid metal from electric current and heat from electric arc, as a result the hydrodynamic parameters of the liquid metal. It is shown that the most important influence in such DC furnaces play electromagnetic Lorentz force, on the second step heat from electric arc and the joule heat in the liquid metal have not so big influence on the intensity of the vortex flow.

#### Acknowledgments

The research was supported by Russian Science Foundation (project No. 19-79-00118).

#### References

- [1] Nekhamin S M, Lunin A G, Krutyanskii M M, and Filippov A K 2005 DC arc melting furnaces *Refractories and Industrial Ceramics* **46** p 37-39

- [2] Kazak O and Semko O 2011 Electrovortex motion of a melt in dc furnaces with a bottom electrode *Journal of engineering physics and thermophysics* **84** p 209-218
- [3] Kazak O and Semko O 2011 Modelling magnetohydrodynamic processes in DC arc steel making furnaces with bottom electrodes *Ironmaking and Steelmaking* **38** p 353-358
- [4] Zaycev V A and Medovar L B 2009 Bottom electrodes of DC arc furnace *SEM* **2** p 3-8 (in Russian)
- [5] Bojarevics V, Freibergs Ya, Shilova E I and Shcherbinin E V 1989 *Electrically induced vortical flows* (Kluwer academic publishers) p 315
- [6] Wang F, Jin Z and Zhu Z 2006 Numerical study of dc arc plasma and molten bath in dc electric arc furnace *Ironmaking and Steelmaking* **33** 39-44
- [7] Henning B, Shapiro M and le Grange L A 2004 DC furnace containment vessel design using computational fluid dynamics *Proceedings: Tenth International Ferroalloys Congress; INFACON X: 'Transformation through Technology'* p 565-574
- [8] Michielan A, Lavaroni G and Fior A 2000 The Danieli Danarc TM furnace *ABS Rev. met.* **6** p 745-752